

# Design Customization and Development of Split Hopkinson Pressure Bar for Light and Soft Armour Materials

Shishay Amare Gebremeskel<sup>1</sup>, Neelanchali Asija<sup>2</sup> and Aryan Priyanshu<sup>3</sup>

<sup>1</sup> Indian Institute of Technology Delhi

*Received: 7 December 2013 Accepted: 4 January 2014 Published: 15 January 2014*

---

## Abstract

In order to face the grand challenge of characterizing soft and light armour material system shaving polymers and shear thickening fluids under impacts at high strain rates lead to design and development of this particular SHPB set up. The developed set up is designed for a maximum firing pressure of 300 bar of nitrogen gas and it comprises automated gas filling and firing, striker bar velocity recording and data acquisition system. Pressure bars are made of titanium alloy due to its high yield strength and reasonably lower density which could protect plastic deformation, wave dispersion and reduces impedance mismatch with the intended soft specimens, unlike maraging steel bars. The maximum stresses on the critical parts of the setup are crosschecked with simulation results and compared with corresponding yield strengths. Velocity-pressure calibration of the developed setup shows higher velocities can be achieved at any particular pressure, when it is compared with the existing public domain velocity calibration of SHPB setup.

---

**Index terms**— split hopkinson pressure bar, high strain rate impact, armour, customized design, simulation.

? Particular SHPB is developed for impact characterization of soft and light materials.

? FEM simulation is done for the critical parts of the setup.

? Hydraulic momentum arrest is provided to avoid repeated loading of specimens.

? Isolation of launching unit vibration is provided to eliminate noise signals.

? Velocity-pressure calibration is performed. Introduction n increasing demand of high strength, lightweight and soft armour material systems, especially for military applications, resulted in interesting research challenge to characterize possible materials at ballistic impacts. Nowadays FRPs and STFs are the main materials of emphasis as a solution for the mentioned challenge. Thus, their high strain rate impact behaviours need to be studied, since their properties at static loadings could not be employed for dynamic designs. For this reason, having an appropriate test setup is significant and SHPB is a potential set up to be used, Jadhav [1]. Since available SHPB setups are designed for particular challenges in terms of capacity, material type and other requirements, design customization and development of own setup for soft materials is found to be necessary.

## 1 Abbreviations

Thus, studying the historical background in advancements of SHPB set up starting from its first innovation up to the latest customizations is important for this particular design. According to studies in [2][3][4][5] Bertram Hopkinson primarily developed a set up called HPB in 1914 using a single bar and its modification was made in 1948 in which electrical equipment was incorporated to record the stress waves. Following this modification, Herbert Kolsky split the HPB in to incident and transmission bars in 1949 and hence the name SHPB. It is this Split Hopkinson Pressure Bar set up that has been widely used in many research studies to characterize materials at dynamic loadings. Articles [6][7][8][9][10][11][12][13] addressed a common design theory for any customization of SHPB design that could result in acceptable calibration curves and stress wave shapes. T he customization

43 made by Robertson et al. [14] is one of the advancements that enabled the setup to test materials at strain rates  
 44 ranging 50 to 104 s<sup>-1</sup>. In a more suitable approach, Haines et al. [9] followed two design phases as mechanical  
 45 system and DAQ system. The mechanical system includes the launching unit which has the high pressure cylinder  
 46 as a main part, the bar) and the momentum arrest. The DAQ system includes the strain gauges, oscilloscope  
 47 and computer as per Guedes et al. [15].

48 To design the pressure bars, more emphasis should be given to the extent of stress waves to be propagated  
 49 through and the following governing equations for strain rate ( $\dot{\epsilon}$ ), strain ( $\epsilon$ ) and stress ( $\sigma$ ) on specimen to be  
 50 tested on the setup are used, Akil [2] and Song & Chen [16]:  $\dot{\epsilon}(t) = \frac{2C_b L_s}{L_s} \dot{\epsilon}_i(t)$ ,  $\epsilon(t) = \frac{2C_b L_s}{L_s} \epsilon_i(t)$   
 51  $(t)dt$ , and  $\sigma(t) = E_b A_b A_s \dot{\epsilon}(t)$

52 Where,  $C_b$  is the elastic wave velocity in the bar,  $L_s$  is the sample length and  $A_s$  and  $A_b$  are the specimen  
 53 and bar cross-sectional areas respectively.  $\epsilon_i$ ,  $\epsilon_r$  and  $\epsilon_t$  are incident, reflected and transmitted strains  
 54 measured from strain gages on the bar, respectively. The pressure bars are of the same material having elastic  
 55 modulus  $E$ , density  $\rho$ , same cross sectional area  $A_b$ , and hence same elastic wavevelocity  $C_b = \sqrt{E/\rho}$ .

56 Since the conventional SHPB setup has been designed for testing hard and metallic materials it is not suitable  
 57 for softer materials like polymers and STFs. Thus, newly customized SHPB setup has to be designed depending  
 58 on the nature of the planned test specimen and expected maximum impact velocity. As part of the customization  
 59 process, selection of material for the pressure bars is very important as the stress wave transmission is highly  
 60 dependent on it. Even though polymeric and aluminium bars are found to be suitable for the stated softer  
 61 materials in terms of impedance matching as per Meng & Li [17] and Butt & Xue [18], the viscoelastic behaviour  
 62 causing wave dispersion and plastic deformation of both these bar materials made them unfit for higher velocity  
 63 impacts. To overcome the stated drawbacks of polymer and aluminum bars, titanium bars are employed in this  
 64 particular design as it has higher yield strength with high elastic deformation behavior at impacts of extreme  
 65 speeds. This study presents the mechanical design analysis of main parts of customized SHPB, where the critical  
 66 ones are supported and validated by FEM simulation using Abaqus CAE.

67 The current design has the following specifications that made it suitable to test softer materials at higher  
 68 strain rates; (a) Pressure cylinder designed to accommodate extreme pressure up to 300 bar of nitrogen gas. (b)  
 69 Automated control of gas filling, firing and instantaneous striker bar velocity recording. (c) Separate foundation  
 70 and construction of the pressure cylinder to isolate the vibration in order not to get transmitted to the bars  
 71 which otherwise would create more noise signals. (d) Complete arrest of momentum using hydraulic momentum  
 72 trapping system. (e) Slender titanium alloy (ASTM Grade-5) bars with diameter of 12 mm having reasonably  
 73 lower acoustic impedance suitable for high strain rate impact testing of softer materials. (f) Negligible friction  
 74 between bars and bearings, by using custom designed adjustable threepoint miniature ball bearings. (g) Simplified  
 75 axis alignment provisions. The overall work is presented in the following chapters.

## 2 II.

77 Materials and Methods a) Design of launching unit, the bars and momentum trapping i. Design of high pressure  
 78 gas cylinder Using the design procedures of pressure vessel:

79 From theory of elasticity according to Budynas & Nisbett [19], a pressure vessel experiences three simultaneous  
 80 principal stresses as shown in Fig. 1. The stresses over the pressure vessel wall are function of radius.

81 Principal stresses;  $\sigma_1 = \sigma_t$  (tangential stress or hoop stress),  $\sigma_2 = \sigma_r$  (radial stress),  $\sigma_3 = \sigma_l$  (longitudinal  
 82 stress). Thick-wall theory is considered, as it is used for any wall thickness-to-radius ratio. Cylinder geometry  
 83 includes  $r_i$ ,  $r_o$  and  $L$  (internal radius, outer radius and length respectively). Cylindrical stresses representing  
 84 the principal stresses,  $\sigma_t$ ,  $\sigma_r$  and  $\sigma_l$ , can be calculated at any radius 'r' in the range of wall thickness between  
 85  $r_i$  and  $r_o$ .

## 3 Global Journal of Researches in Engineering

87 Tangential or hoop stress can be given as;  $\sigma_t = \frac{P_i r_i^2 + P_o r_o^2 + r_i^2 r_o^2 (P_o - P_i)}{r^2 r_o^2 - r_i^2}$ ;  $r_i < r < r_o$   
 88  $\sigma_r$  (1)

89 and similarly the radial stress can be given;  $\sigma_r = \frac{P_i r_i^2 + P_o r_o^2 + r_i^2 r_o^2 (P_o - P_i)}{r^2 r_o^2 - r_i^2}$ ;  $r_i < r < r_o$   
 90  $\sigma_l$  (2)

91 However, the longitudinal stress is applicable to cases where the cylinder carries longitudinal load, such as in  
 92 capped ends and in boiler vessels, valid where bending, nonlinearity and stress concentrations are not significant  
 93 and can be estimated as;  $\sigma_l = \frac{P_i r_i^2 + P_o r_o^2 + r_i^2 r_o^2 (P_o - P_i)}{r^2 r_o^2 - r_i^2}$ ;  $r_i < r < r_o$  (3)

94 Two mechanical design cases can be considered as; Case-1: internal pressure only ( $P_o = 0$ )

95 Case-2: external pressure only ( $P_i = 0$ ) This particular design of high pressure gas container corresponds to  
 96 the first case, where  $P_o = 0$ ; therefore, the critical section exists at  $r = r_i$ , for which the hoop stress can be  
 97 evaluated as;  $\sigma_t(r = r_i) = \sigma_{t,max} = \frac{P_i r_o^2 + r_i^2 r_o^2}{r_i^2} = \frac{P_i}{2} \left( \frac{r_o}{r_i} + 1 \right)^2$  (4)

98 Where,  $\sigma_l = \frac{r_o}{r_i} \sigma_{t,max}$  (5)  $\sigma_l = \frac{P_i}{2} \left( \frac{r_o}{r_i} + 1 \right)^2$  (6)

99 are function of cylinder geometry only.

100 And the radial stress will become;  $\sigma_r(r = r_i) = \sigma_{r,max} = \frac{P_i}{2}$  (which is a natural boundary condition) (7)

101 The longitudinal stress depends on end conditions:  $\sigma_l = \frac{P_i C_{li}}{L}$ , capped ends 0, uncapped ends (8)

102 Where,  $C_{li} = 1$  for uncapped ends (9)

---

103 For calculating the thickness 't' of the cylindrical shell [20], the following equation can be used. $t = P \cdot r \cdot i \cdot SE$   
104  $0.6P \cdot i \cdot (10)$

105 Where,

## 106 4 S(allowable design stress) =

107 ? yt FOS (11) The dimensions of the designed pressure cylinder are given in Fig. 2. The high pressure gas  
108 cylinder is subjected to thrust force generated after each firing process. This thrust force will be transmitted to  
109 its column. Fig. ?? shows the dimensions of the column and point of application of the transmitted thrust force.

## 110 5 Fig. 3 : FBD of pressure cylinder column

111 The maximum thrust force  $F_t$  that this part can face is dependent on the net drop of the cylinder pressure after  
112 single firing. $F_t = P_{net} \cdot A_{bore}$  (12)

113 Where,  $P_{net}$  is the net drop of the pressure at single firing  $A_{bore}$  is cross sectional area of the cylinder bore  
114 Using the formula for design or allowable bending stress  $\sigma_b : \sigma_b = M / Z$  (13)

115 Where,  $M$ = bending moment and  $Z$ = section modulus  $M = F_t \cdot L$ , length  $L$  of the column is fixed by the  
116 axis height of the set up to be 800 mm. Internal diameter ID of the column is fixed by the swivel of the thrust  
117 bearing seat to be 75 mm and the outer diameter OD to be calculated. To avoid buckling of the bars in between  
118 the supports, most literatures recommend that their aspect ratio ( $L/D$  ratio) should be limited to 100, however  
119 with three-point contact miniature ball bearings (float bearing) having low coefficient of friction can be used  
120 to increase the  $L/D$  ratio. As shown in Fig. 5, the length  $L$  of the bars is maintained to be 1200 mm while their  
121 diameter is fixed by striker bar to be 12mm.

## 122 6 Design of bars and barrel

## 123 7 Position of bearing supports of Incident and Transmission 124 bars

125 The number of bearing supports 'n' is fixed to be two for each bar and their position is calculated by using Airy's  
126 formula [21]. Considering the barrel as a short time pressure vessel with no welded joints; corresponding joint  
127 efficiency,  $E$ , is given as 1 and FOS is fixed to be 2. Its thickness 't' is calculated using the formula in equation (  
128  $??0$ ) above as the internal radius of the barrel 'r<sub>ib</sub>' is fixed by the radius of the striker bar to be 6mm.

129 The necessary dimensions are accordingly calculated and given in Fig. 7. Selection of the right hydraulic oil  
130 should be made based on its bulk modulus or compressibility. For complete absorption of the kinetic energy KE  
131 generated at 300 bars of reservoir pressure and safe design, we assume that the total KE of the striker bar at  
132 its maximum velocity of 600m/s will be transferred to the momentum trap. From Fig. 8 it is observed that the  
133 level  $H$  of oil responsible to absorb the momentum is made 160mm and an initial volume  $V_o$  is calculated as;  
134  $V_o = \pi \cdot d_i^2 \cdot H$  (21)

135 Allowing 0.2 % change in volume  $\Delta V$  of the oil, bulk modulus  $E$  of the hydraulic oil will be calculated as;  
136  $E = \Delta KE / \Delta V$  (22)

137 According to the technical data in [22] the possible oil at 300 bar pressure is the petroleum based hydraulic  
138 oil with corresponding bulk modulus  $E$  of 1.6 GPa is therefore selected.

139 Considering the momentum trap as a mass attached with a spring and damper as shown in Fig. 9, it is  
140 modeled and the stiffness and damping coefficient are predicted as follows; $F_d + Kx + Cv = 0$ (23)

141 Where,  $F_d$  is the maximum dynamic force to be trapped,  $K$  is the stiffness of the momentum trap,  $x$  is the  
142 maximum axial displacement of the piston,  $C$  is the damping coefficient of the momentum trap and  $v$  is velocity  
143 of the striker bar. The stiffness  $K$  is calculated using the following formula; $K = m \cdot \omega_n^2$  (24)

144 Where,  $m$  is mass of the movable parts in the momentum trap (head+rod+piston), and  $\omega_n$  is the natural  
145 frequency. $\omega_n = C_{st} / 2 \cdot L_t$  (25)

146 where  $C_{st}$  is speed of sound in the bars given as 5073 m/s and  $L_t$  is length of the transmission bar.

## 147 8 III.

### 148 Fem Simulation of Critical Parts using Abaqus cae 6.10 a) Pressure Cylinder

149 The following input data are provided to simulate the stress condition of the cylinder under maximum nitrogen  
150 gas pressure and observation of the maximum stress is taken, as shown in Fig. 10 Loading Duration = 60 ?s  
151 (set to be two times period of the wave to check for higher stress) Since each bar of the assembly could not be  
152 visually identified in a window at a time, the zoomed images of the interaction areas are displayed in Fig. 12.  
153 The first one is the interaction between striker bar and incident bar while the second one is between incident bar,  
154 specimen and transmission bar. The results of which are discussed later in the Results and Discussion section.  
155 The instrumentation of the SHPB set-up typically comprises a velocity measurement system, strain gauges, high  
156 speed strain gage input module with builtin signal conditioner and amplifier as well as voltage excitation source  
157 for powering the wheat stone bridge circuit, and oscilloscope for the display of acquired strain signals in both the

158 incident and transmission bars. The following section discusses each of the above components of DAQ system in  
 159 detail.

160 **9 i. Velocity Measurement System**

161 The main purpose of the velocity measurement system is to determine the impact velocity of the striker bar. It  
 162 comprises of two IR (Infra-red) sensors, KOYO PLC and high speed counter module (HO-CTRIO-2). As soon  
 163 as the striker bar is triggered, it passes in front of the IR sensors within a fraction of second. Consequently,  
 164 pulse state and stop is registered in the PLC. The function of the high speed counter module is to determine  
 165 the time duration between the consecutive pulse start and stop. By knowing the distance between the speed  
 166 sensors, the impact velocity of the striker bar is calculated. The schematic of the velocity measurement system  
 167 is illustrated in Fig. 13. This system comprises of the strain gages, signal conditioner cum amplifier and data  
 168 acquisition (DAQ) system. The selection of appropriate DAQ system is solely based upon the required sampling  
 169 frequency (f s ) i.e. number of samples taken per second. The sampling rate of the DAQ system must satisfy the  
 170 Nyquist criterion [23], which states that the signal must be sampled at a frequency which is greater than twice  
 171 the highest frequency component of interest in the signal, otherwise, the high frequency content will alias at a  
 172 frequency inside the spectrum of pass-band. The specific DAQ system used in this setup is based on NI PXIe  
 173 supported by Lab view software. Fig. 14 shows the photograph of the DAQ and analysis system including the  
 174 strain input card and the monitor. Sampling rate f s of the DAQ system  $T = \lambda / C$  (26)

175 Where,  $\lambda$  is the wave length and C is the wave speed with in the pressure bars. The wave length  $\lambda$  is two  
 176 times the length of the striker bar which comes out to be 0.152m (2\*0.076m). Period T is calculated to be 30  $\mu$ s  
 177 and the subsequent maximum wave frequency f max will be 1/T, which is nearly 34 KHZ. Thus, sampling rate of  
 178 DAQ system, according to Nyquist criteria; f s > 2f max , should at least be 70 Kilo samples per second (>2\*34  
 179 KS/sec).

180 **10 Wheatstone Bridge Configuration**

181 Two active strain gages were mounted diametrically opposite on the bars, thus constituting Half Bridge Type II  
 182 configuration. In Fig. 15, R 1 and R 2 are the half bridge completion resistors, R 3 is the active strain gage  
 183 element measuring the compressive strain (- $\epsilon$ ) and R 4 is the active strain gage element measuring the tensile  
 184 strain (+ $\epsilon$ ). This bridge configuration measures purely axial strain while rejecting the bending strain. The strain  
 185 gage output voltage was converted to corresponding strain units by using the following equation. Strain ( $\epsilon$ ) = (  
 186  $\frac{V_r}{V_{EX}} - 1$ ) \*  $\frac{R_g}{R_L + R_g}$  (27)

187 Where, V r (the voltage ratio) =  $\frac{V_{CH}}{V_{EX}}$  (28)  
 188 V EX is the excitation voltage, V CH is the measured signal voltage, GF is Gage factor of the strain gages and  
 189 R L & R g are lead resistance and nominal strain gage resistance, respectively.

190 **11 e) Fabrication and Installation**

191 Fabrication of the designed SHPB parts, their assembly and the total installation is thereby accomplished. The  
 192 total setup assembly contains different mechanical, electrical and electromechanical parts as tabulated in Table  
 193 1 below. ? High pressure gas reservoir (300 bar capacity)  
 194 ? Reservoir vent needle valve (250 bar capacity)  
 195 ? Reservoir column  
 196 ? Swivel  
 197 ? Nitrogen gas supply pressure cylinder (accumulator)  
 198 ? High pressure nipples (400 bar capacity)  
 199 ? High pressure Union pipe joints (250 bar capacity)  
 200 ? Barrel support block-1 (large)  
 201 ? Barrel support block-2 (small)? Barrel clamps (2)  
 202 ? Cross channels (2)  
 203 ? Bearing supports (4)  
 204 ? Floater bearings (4)  
 205 ? C-clamps (18)  
 206 ? Hydraulic momentum trap The solid model and photograph of the developed setup are shown in Fig. 16  
 207 and Fig. 17 respectively, which is in effect developed from scratch and will give an idea to others to create it  
 208 from a junk yard. ?

209 **12 Results and Discussion**

210 From the start of the design, assumptions of perfect gas law and adiabatic expansion were considered to make  
 211 use of maximum pressure energy for safe design of the parts of the setup. The maximum pressure of nitrogen  
 212 gas with in the cylinder which is 300 bar is considered throughout the entire design of each component part.  
 213 Accordingly, every part of the setup is shown to be safe against the maximum applied stress. The main parts are  
 214 summarized and listed in Table 2 for comparison of their strength with the maximum possible stresses obtained  
 215 in FEM simulation as well as analytically. As presented in Table 2 above, the maximum possible stresses in each

216 part as a result of design and simulation are reasonably close to each other and less than the corresponding yield  
217 strengths, which shows a safe design, however, the stress in pressure bars is quite close to the yield strength and  
218 may require continuous observation of their ends for any plastic deformation.

219 The one dimensional stress S-33 propagation along the axial direction (Z-axis) of the pressure bars is shown  
220 by post process in Fig. 18. For visualization purpose, around half the length of the incident bar is taken and  
221 the graph is displayed in five even and successive step time frames namely S33\_T1, S33\_T2, S33\_T3, S33\_T4  
222 and S33\_T5. Since the time period is set to be 100 $\mu$ s, each step frame occurs at every 20  $\mu$ s. It can be observed  
223 that the maximum stress on the pressure bars during such a very short loading duration is a compressive stress  
224 just exceeding 700 MPa in all the time frames. The exact value of this maximum stress can be seen in Fig.  
225 12 and Only one available paper by Haines et al. [9] presented the velocity-pressure curve of SHPB having curve  
226 fitting equation of  $v = 7.9507p - 0.2387$ . In this work the curve fitting equation shown in the above graph is  
227 about 3.5X steeper. That means the velocity of the striker bar of this design is 3.5 times more at the same firing  
228 pressure. Moreover, the regression parameter R<sup>2</sup> is close to one which indicates consistency of the nitrogen gas  
229 expansion, negligible gas leakage through the joints, proper propelling barrel length and size of striker bar.

### 230 13 V. Conclusion

231 Development of particular SHPB set up of length 6.5m, height 1.2m and width of 0.56m is done after necessary  
232 design analysis and overall customization in house. This set up mainly focuses for high strain rate impact  
233 characterization of soft and light armor material systems like polymers and FRPs. Parts of the setup are designed  
234 for the maximum firing pressure of 300 bar with slender titanium bars of 12 mm diameter to help the assumption  
235 of one dimensional stress wave propagation theory. The launching unit is made separated by foundation from  
236 the bars table to protect the vibration noise signals not to be transmitted to the pressure bars. Mechanism for  
237 floater bearings is also developed to reduce the coefficient of friction which could happen between the bearing-  
238 bar interactions. A hydraulic momentum trap is provided to avoid repeated loading of test specimens so that  
239 the specimen could further be examined by subsequent tests like scanning electron microscopy. The maximum  
240 stresses on the critical mechanical parts of the setup; the cylinder, column and bars were cross checked with the  
241 FEM simulation results and compared with its corresponding yield strengths, hence safe design of the setup is  
242 observed. The velocity-pressure calibration graph achieved in this design shows that the velocity of the striker bar  
243 at a particular pressure is about 3.5 times more than the one presented in previous works. Testing of polymers  
244 and composites is in progress using this newly developed setup.

VI.



Figure 1: Fig. 1 :

245

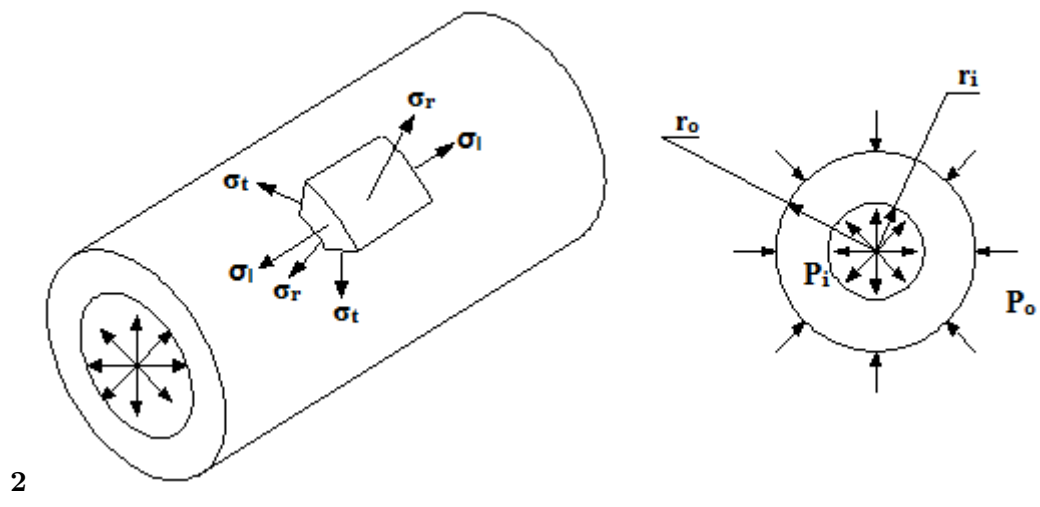
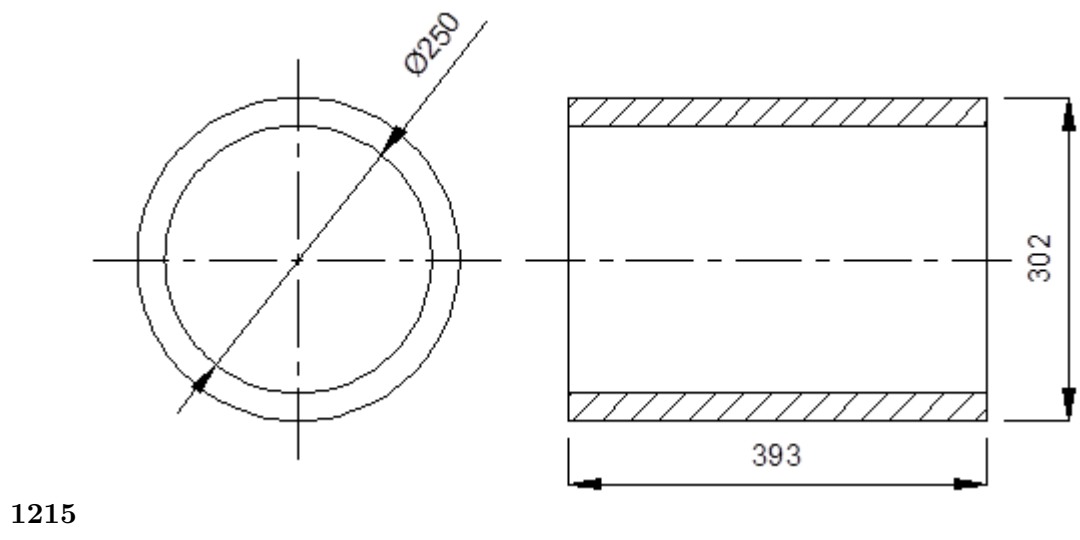


Figure 2: Fig. 2 :



1215

Figure 3: 1 2 m s V s 2 ( 15 )

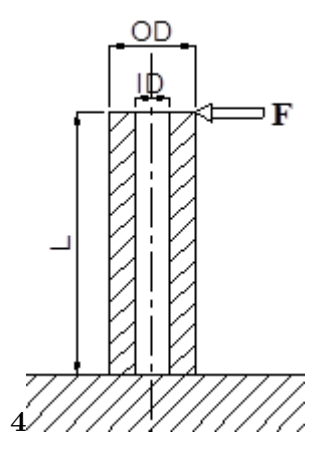


Figure 4: Fig. 4 :

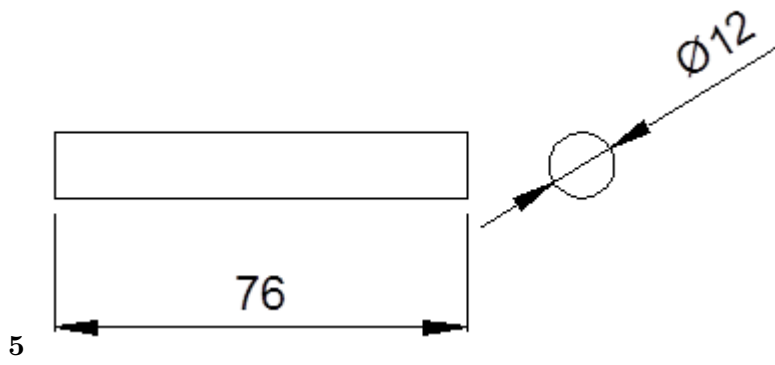


Figure 5: Fig. 5 :

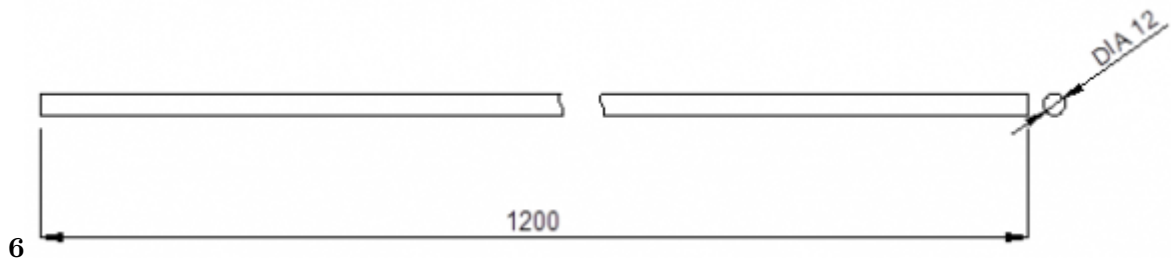


Figure 6: Fig. 6 :

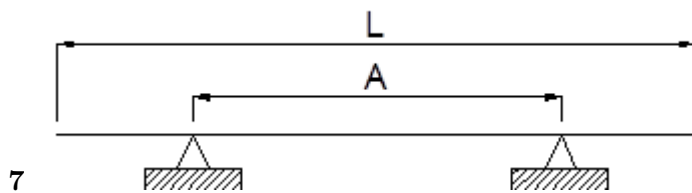


Figure 7: Fig. 7 :

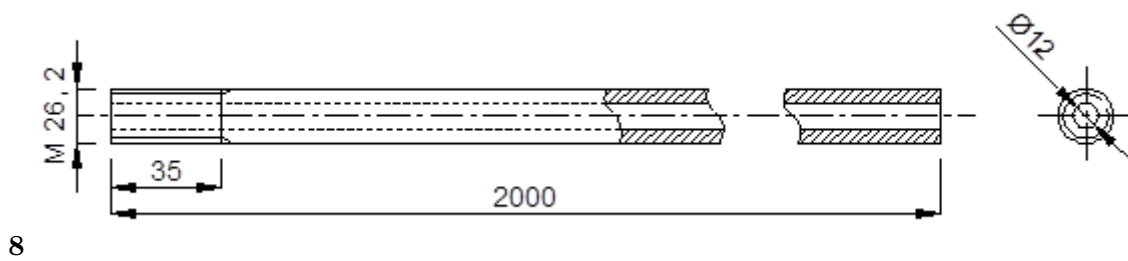
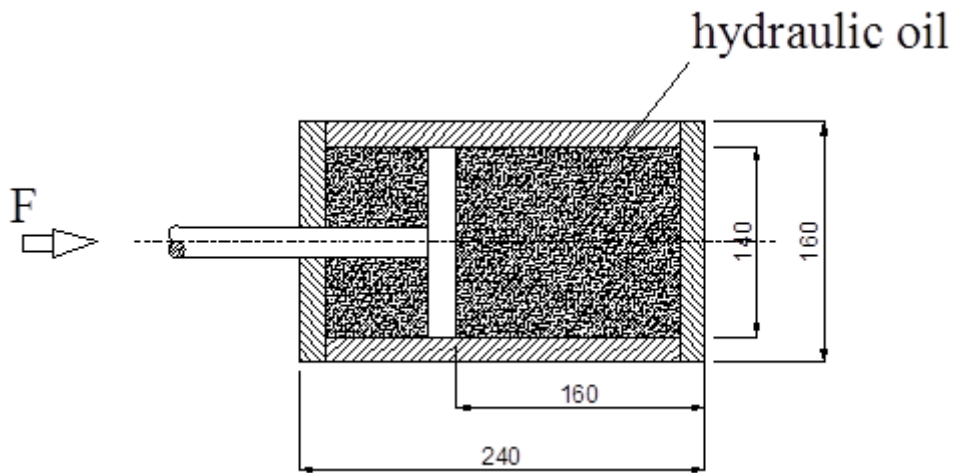
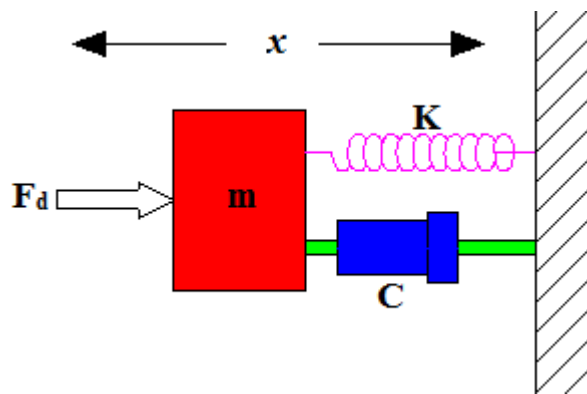


Figure 8: Fig. 8 :



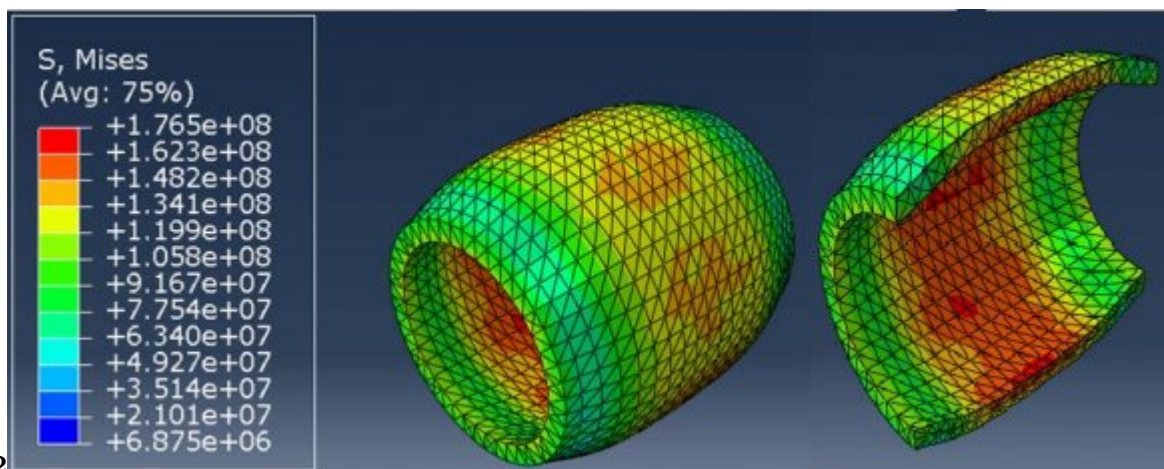
9

Figure 9: Fig. 9 :



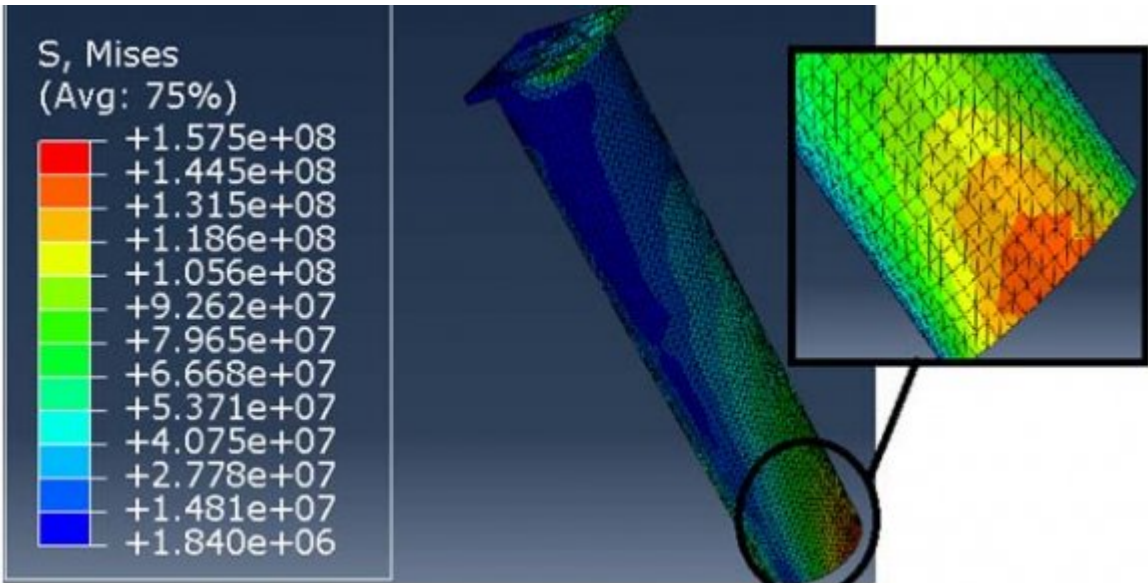
1011

Figure 10: Fig. 10 :Fig. 11 :



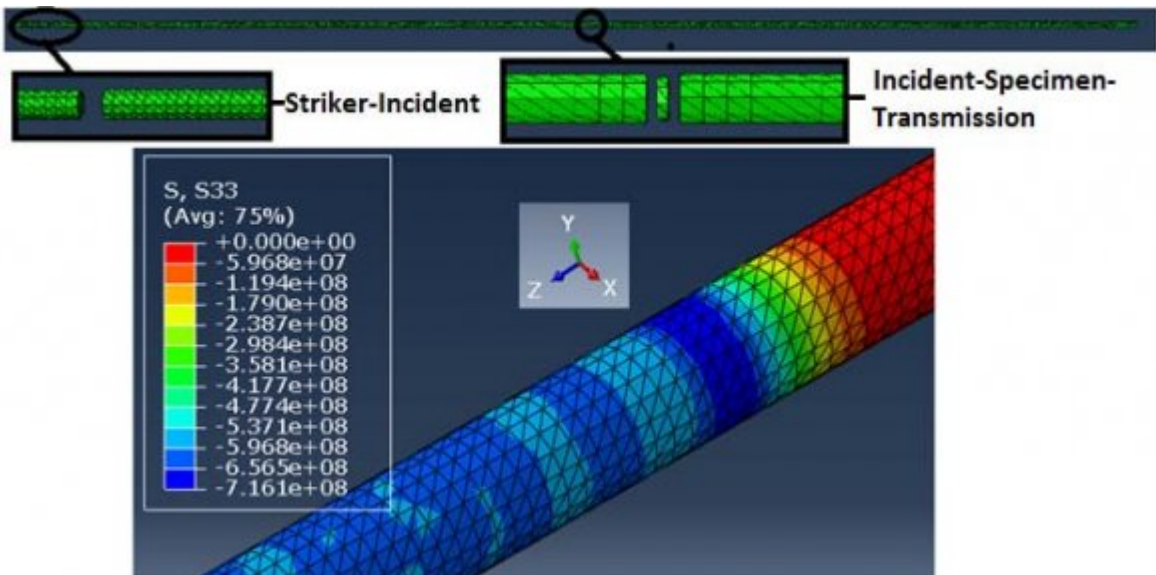
12

Figure 11: Fig. 12 :



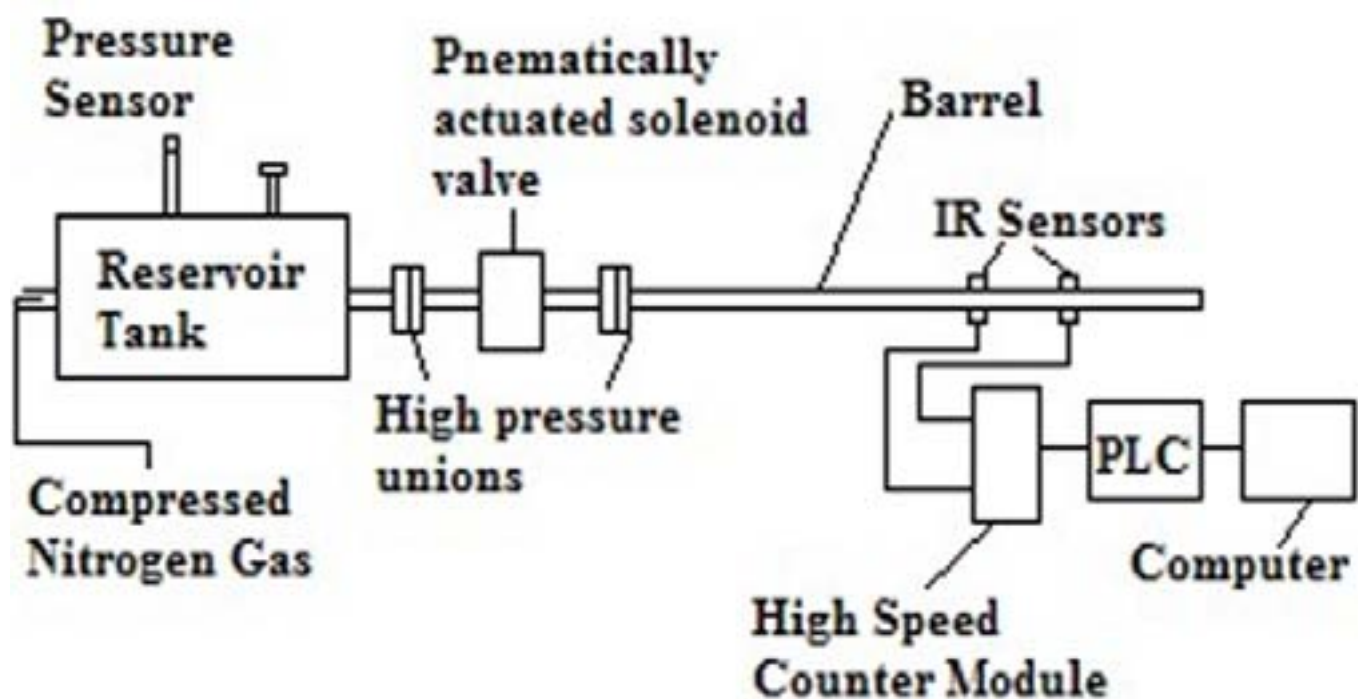
13

Figure 12: Fig. 13 :



14

Figure 13: Fig. 14 :



15

Figure 14: Fig. 15 :

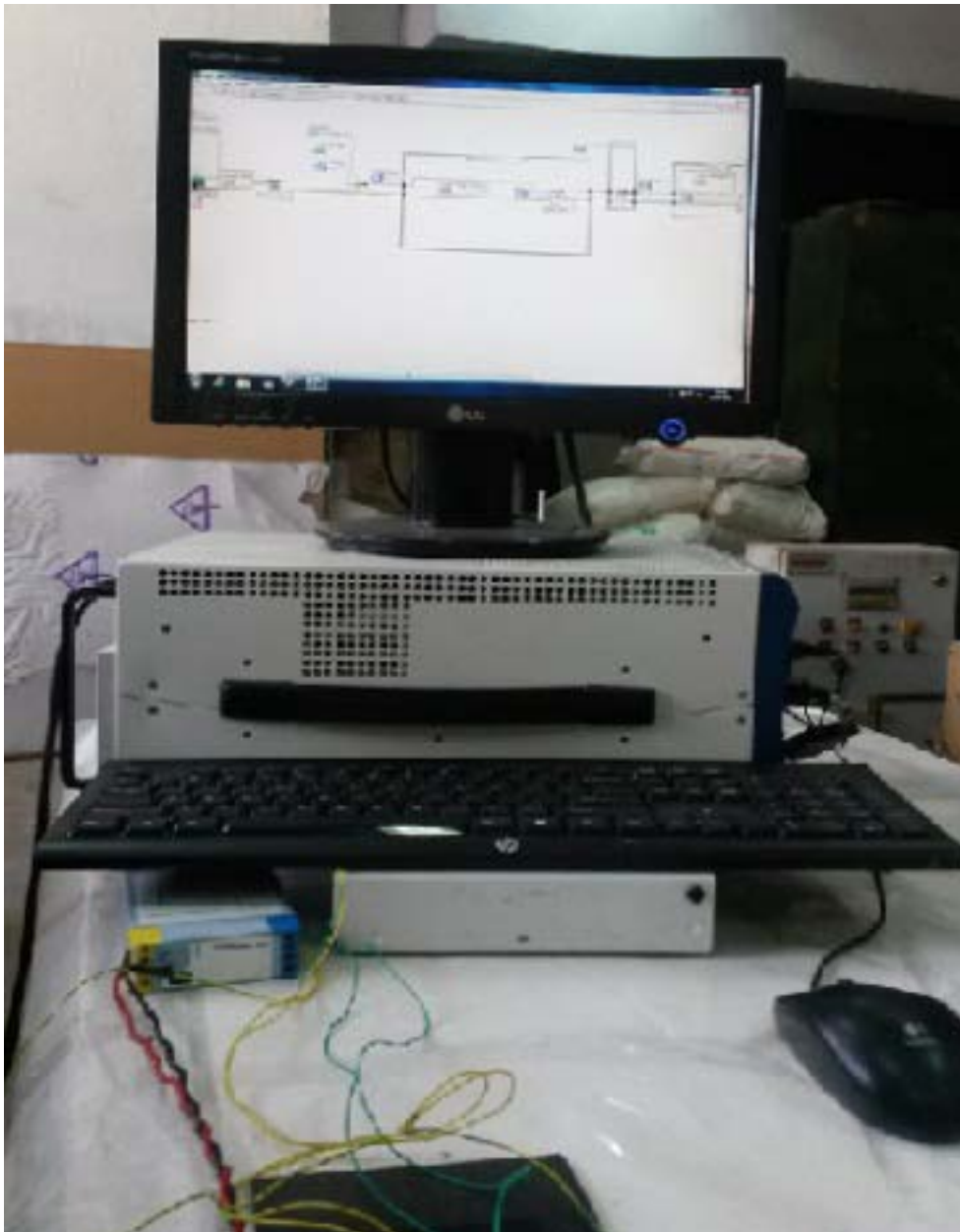
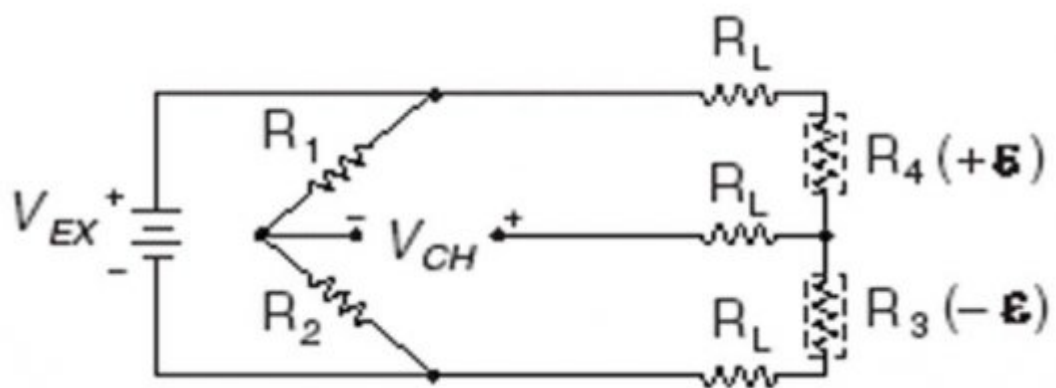


Figure 15: ??



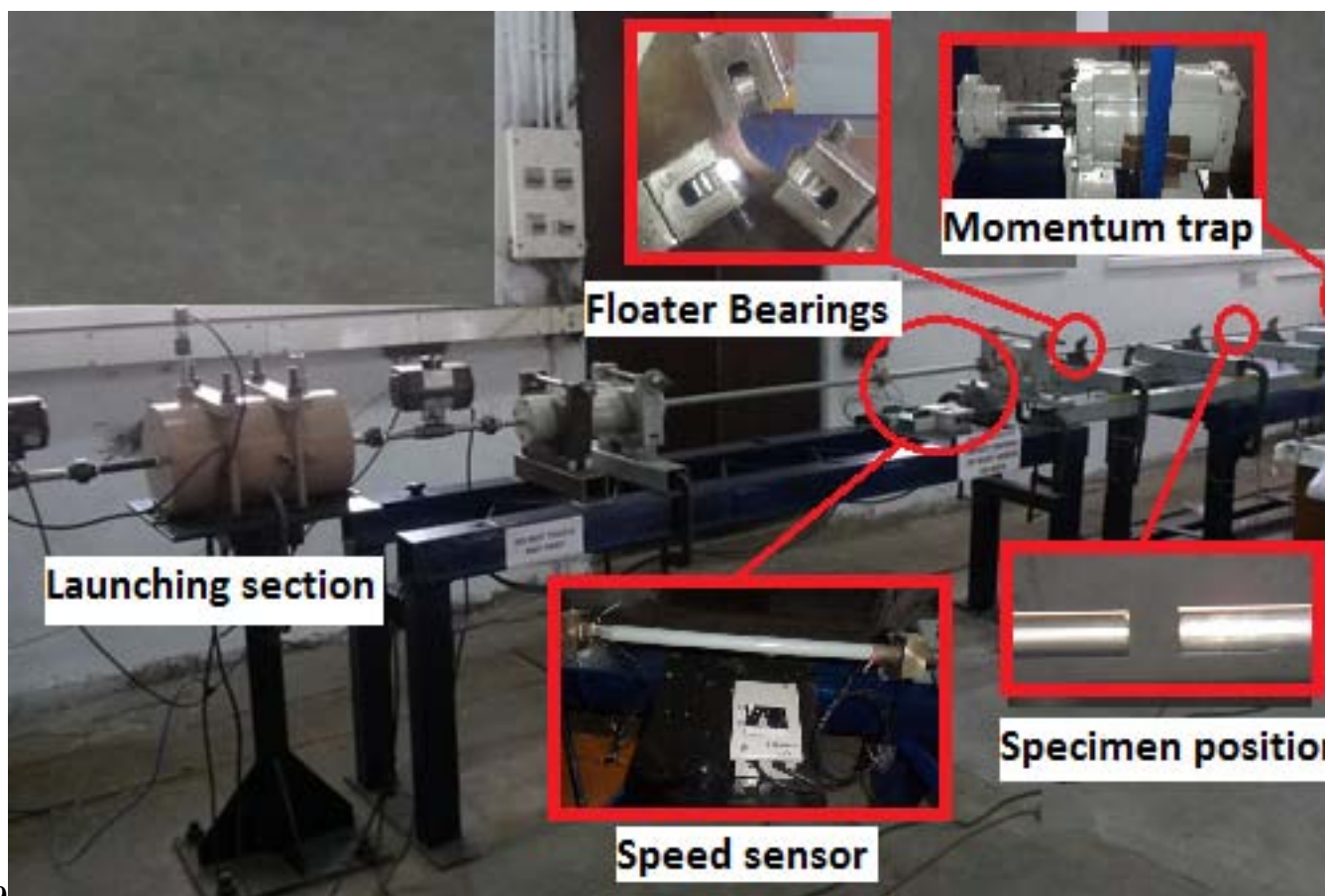
16

Figure 16: Fig. 16 :



17

Figure 17: Fig. 17 :



1819

Figure 18: Fig. 18 :Fig. 19 :

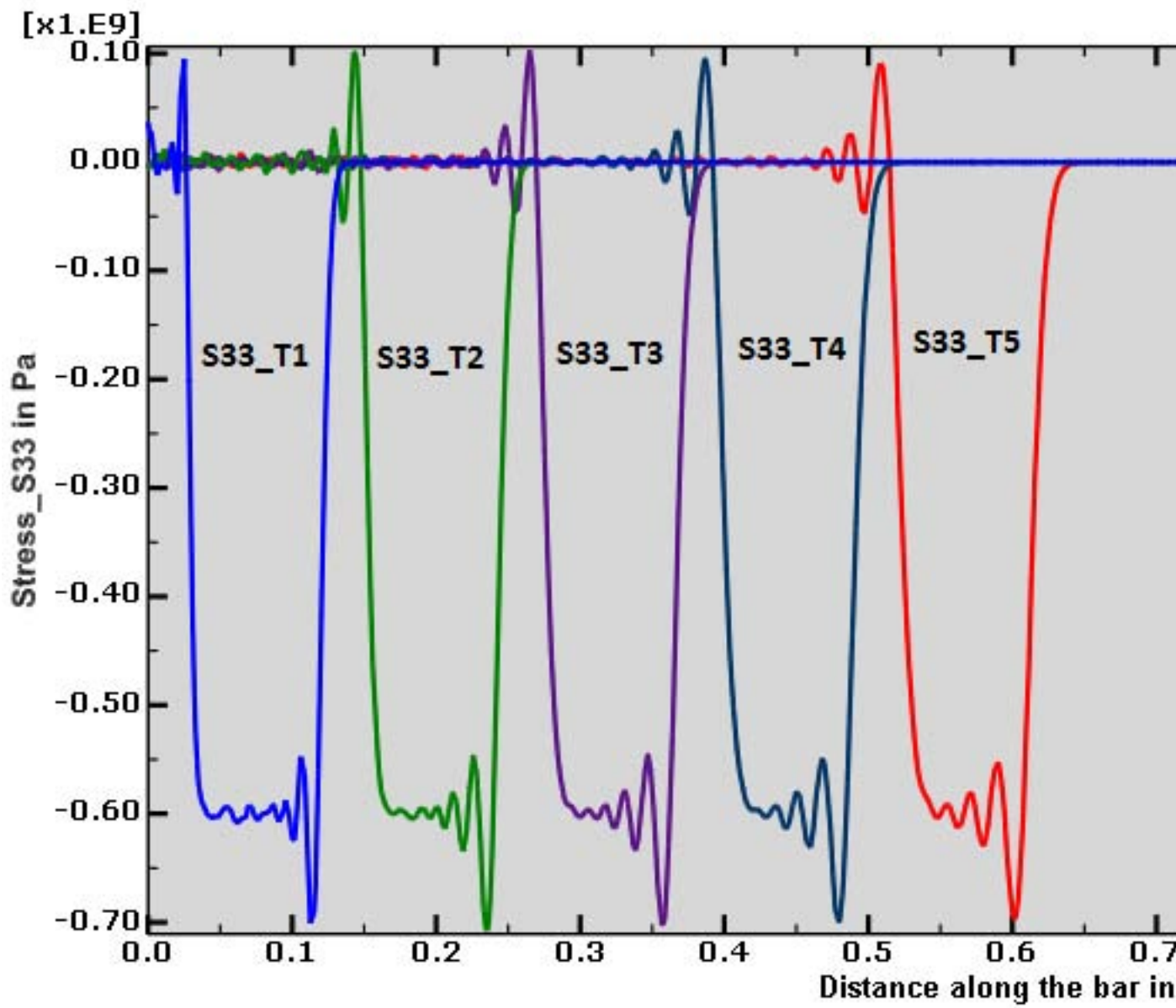


Figure 19:

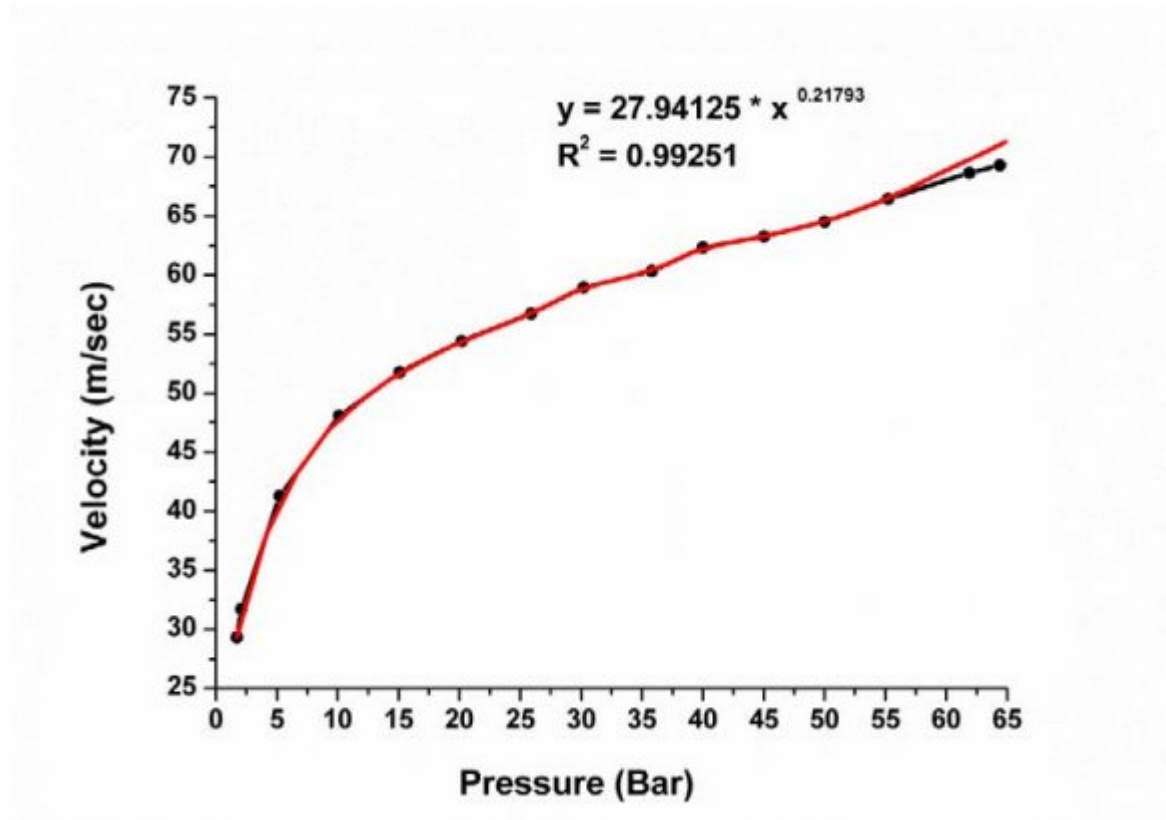


Figure 20:

1

List of Split Hopkinson Pressure Bar Parts  
Mechanical parts

Electrical and Electromechanical Parts

? Base tables

Figure 21: Table 1 :

2

| Strength and Stresses          | Pressure Cylinder<br>(AISI4130, steel) | Column of Cylinder<br>(AISI4130, steel) | Pressure Bars<br>(Ti6Al4V) |
|--------------------------------|----------------------------------------|-----------------------------------------|----------------------------|
| Yield Strength(δ ??”δ ??” ?? ) | 460 MPa                                | 460 MPa                                 | 830 MPa                    |
| Max. Stress (by design)        | 160.5 MPa                              | 230 MPa                                 | 796.2 MPa                  |
| Max. Stress<br>(bysimulation)  | 176.5 MPa                              | 157.5 MPa                               | 716 MPa                    |

Figure 22: Table 2 :

2

as 716MPa

Figure 23: Table 2

.1 Acknowledgement

- 246 The authors are indebted to IRD-IITD for a grand challenge grant (MI00810) for doing this research project.  
247  
248 [Gama et al. ()] , B A Gama , S L Lopatnikov , J W Gillespie . *Hopkinson Bar Experimental Technique: A*  
249 *critical Review. ASME Appl. Mech. Rev* 2004. 57 (4) .  
250 [Airy Points (2013) The Engineer’s Notebook] *Airy Points (2013) The Engineer’s Notebook*,  
251 [Meng and Li ()] *An SHPB setup with reduced time-shift and pressure bar length. IJIE*, H Meng , Q M Li . 2003.  
252 28 p. .  
253 [Haines et al. ()] *Design and Characteristics of a Split Hopkinson Pressure Bar apparatus*, J Haines , C Knight  
254 , R Glaser . 2007. Dept. Mech. Eng., Univ. of Maine  
255 [Robertson et al. ()] *Design and operating characteristics of a Split Hopkinson Pressure Bar Apparatus. Army*  
256 *materials and mechanics research center, Mechanics of materials division*, K D Robertson , S C Chou , J H  
257 Rainey . AMMRC TR/1-49. 1971. W. Massachusetts.  
258 [Lang ()] *Design of a Split Hopkinson Bar Apparatus for use with Fiber Reinforced Composite Materials*, S M  
259 Lang . 2012. Logan, Utah. Dept. Mech. Eng., Utah State Univ. (M.S. thesis)  
260 [Gallina et al.] *Design of a Split Hopkinson Pressure Bar*, F Gallina , R S Birch , M Alves . Brazil. Univ. of Sao  
261 Paulo (Unpublished results)  
262 [Butt and Xue ()] *Determination of the wave propagation coefficient of viscoelastic SHPB: Significance for*  
263 *characterization of cellular materials*, H S U Butt , P Xue . 2013. (IJIE)  
264 [Owens ()] *Development of a Split Hopkinson Tension Bar for testing stress-strain response of particulate*  
265 *composites under high rates of loading*, A T Owens . 2007. Alabama. Auburn Univ. (M.S. thesis)  
266 [Chen et al. ()] ‘Dynamic Compression Testing of Soft Materials’. W Chen , F Lu , D J Frew , MJ . *ASME*  
267 *Journal of Appl. Mech* 2002. 69 p. .  
268 [Huang ()] *Dynamic testing of soft and ultrasoft materials*, S Huang . 2009. Dept. Civ. Eng., Univ. of Toronto  
269 (M.S. thesis)  
270 [Ramesh ()] *High Strain Rate and Impact Experiments*, K T Ramesh . 2008. Springer. (Experimental Solid  
271 Mechanics)  
272 [Jadhav ()] *High strain rate properties of polymer matrix composites*, Jadhav . 2003. Univ. of Pune (M. S. thesis)  
273 [Yokoyama] ‘Prediction of Maximum Strain and Strain Rate in SHPB Specimens Based on Energy Analysis’. T  
274 Yokoyama . *Okayama Univ. of Science* (Unpublished results)  
275 [O ()] *Quasi-Static and High Strain-Rate Mechanical Behavior of FP? (?-alumina) Long Fiber Reinforced*  
276 *Magnesium and Aluminum Metal Matrix Composites*, O . 2004. Dept. Materials Science & Eng., Izmir Inst.  
277 of Tech., Turkey (M.S. thesis)  
278 [Guedes et al.] *Response of CFRP Laminates under High Strain Rate Compression until Failure*, R M Guedes ,  
279 M A Vaz , F J Ferreira , J L Morais . Portugal. (Unpublished results)  
280 [Sauer-Danfoss ()] Sauer-Danfoss . *Hydraulic fluids and lubricants technical information. 520L0463. REV HC*,  
281 2010.  
282 [Lindholm and Yeakley ()] *Split Hopkinson Pressure Bar Apparatus. ASME, Southwest Research Institute*, U S  
283 Lindholm , L M Yeakley . 2006. San Antonio, Texas.  
284 [Song and Chen ()] ‘Split Hopkinson Pressure Bar Techniques for Characterizing Soft Materials’. B Song , W  
285 Chen . *LAJSS* 2005. 2 p. .  
286 [Manual] *Stress in pressure vessels*, Manual . (Unpublished results)  
287 [Budynas and Nisbett ()] ‘Stress in pressurized cylinders’. R G Budynas , J K Nisbett . *Shigley’s Mechanical*  
288 *Engineering Design*, (New York, ch. 3, sec) 2011. McGraw-Hill. p. . (9th ed)  
289 [Tasneem ()] *Study of wave shaping techniques of Split Hopkinson Pressure Bar using Finite Element Analysis*,  
290 N Tasneem . 2002. Dept. Mech. Eng., Osmania Univ., Osmania (M.S. thesis)  
291 [Kester ()] *What the Nyquist criterion means to your sampled data system design*, W Kester . MT-002 tutorial.  
292 2009. (Analog devices)